More evidence for an intracluster planetary nebulae population in the Virgo cluster

R. H. Méndez

Munich University Observatory, Scheinerstr.1, Munich 81679, Germany

M. A. Guerrero

Instituto de Astrofísica de Canarias, E-38200 La Laguna, Tenerife, Spain

K. C. Freeman

Mt. Stromlo and Siding Spring Observatories, Weston Creek P.O., ACT 2611, Australia

M. Arnaboldi

Osservatorio Astronomico di Capodimonte, V. Moiariello 16, Napoli 80131, Italy

R. P. Kudritzki and U. Hopp

Munich University Observatory, Scheinerstr.1, Munich 81679, Germany

M. Capaccioli

Osservatorio Astronomico di Capodimonte, V. Moiariello 16, Napoli 80131, Italy

and

H. Ford

Physics and Astronomy Dept., The John Hopkins University, Homewood Campus, Baltimore, MD 21218, U.S.A.

Received ______________________; accepted ______________________

ABSTRACT

We surveyed a 50 arcmin^2 region in the Virgo cluster core to search for intergalactic planetary nebulae, and found 11 candidates in the surveyed area. The measured fluxes of these unresolved sources are consistent with these objects being planetary nebulae from an intergalactic population of stars, although we cannot exclude some minor contamination of our sample by redshifted starburst galaxies. We compute the cumulative luminosity function of these 11 planetary nebula candidates. If we assume that they belong to the Virgo cluster, their cumulative luminosity function is in good agreement with planetary nebula luminosity function simulations for a typical stellar population of ellipticals or spiral bulges. This comparison allows us to estimate the surface mass density of the intergalactic stellar population at the surveyed field in the cluster core.

Subject headings: galaxies: clusters: individual (Virgo cluster) — galaxies: intergalactic medium — planetary nebulae: general

1. Introduction

A recent study of the dynamics of the outer regions of NGC 4406 (M 86) using radial velocities of planetary nebulae (PNs) by Arnaboldi *et al.* (1996) produced the serendipitous discovery of 3 PNs whose velocities were near the mean redshift of the Virgo cluster (around +1400 km s^{-1}). Since NGC 4406 has a peculiar redshift of about −230 km s^{-1}, this led to the conclusion that the 3 PNs do not belong to NGC 4406, but are members of an intergalactic or intracluster diffuse stellar population in the Virgo cluster. More recently, other independent observations gave further evidence for intracluster stars: a deep HST image of a blank field near M 87 revealed several hundreds of red giants (Ferguson *et al.* 1996, 1997), and Theuns and Warren (1997) reported the detection of several intracluster PN candidates in the Fornax cluster.

The existence of a diffuse intracluster stellar population has been expected, as a consequence of the stripping of stars from galaxies in clusters through the effect of fast encounters with other galaxies and the interaction of the galaxies with the tidal field of the cluster itself. This process (harassment) was simulated recently by Moore *et al.* (1996). Planetary nebulae are ideal tracers of such an intracluster stellar population. They are relatively easy to find and, from surveys of several fields in the Virgo Cluster, it is possible to map the surface density distribution of the intracluster population, compare it with the distribution of the galaxies in the cluster (see Binggeli *et al.* 1987), and estimate its total mass. In addition, the fact that the detected flux is concentrated in one spectral line ([O III] λ5007) makes it relatively easy to measure the radial velocities of these intracluster PNs with adequate accuracy. Using the PN radial velocities, we can compare the kinematics of this intracluster population with the kinematics of the diffuse population produced in simulations of galaxy harassment.

As a by-product of the PN detections, the luminosity function of the intracluster PNs

can be used to obtain a new estimate of the distance to the Virgo cluster, less affected by problems of incompleteness of galactic PN samples and the back-to-front uncertainties related to the galaxy morphological types and their spatial segregation in the cluster (e.g. Jacoby *et al.* 1990). Given a large enough sample of intracluster PNs it will be interesting to compare them with the Jacoby *et al.* (1990) PNs, because the intracluster sample may have slightly brighter PNs; across the cluster depth we expect to detect preferentially those PNs which are closer to us (Jacoby 1997).

To enlarge the statistics on the intracluster PN population in the Virgo cluster core, we decided to survey an additional field in Virgo, using the well-established [O III] on-band/off-band technique of Jacoby *et al.* (1990). We selected a field near the core of the Virgo cluster but well away from bright galaxies and bright stars, and made a deep search for intracluster PNs. In this letter we present the discovery of 11 PN candidates (Sections 2 and 3), and discuss of possible contaminations from starburst galaxies at high redshifts in Section 4. We discuss the cumulative PN luminosity function (PNLF) and the surface mass density of the diffuse population in Sections 5 and 6. Conclusions are given in Section 7.

2. Observations and reductions

The highest priority field for our survey was centered at RA(2000)= $12^h26^m32\overset{s}{.}1$, $\delta(2000) = +12°14'39''$, in the core region, near the center of group A in the Virgo cluster (see the isopleths in Fig. 4 of Binggeli *et al.* 1987), where there are no bright stars and no giant galaxies, in order to survey only the diffuse intracluster population. Using the NED database[1] we verified that there is no known dwarf or low surface brightness galaxy

[1]The NASA/IPAC Extragalactic Database (NED) is operated by the Jet Propulsion Laboratory, California Institute of Technology, under contract with the NASA.

belonging to the Virgo cluster within the selected field. The only previously known galaxy in the field is number 166 in Drinkwater *et al.* (1996), a background object at a redshift $z = 0.0845$. We also verified that an extrapolation of the halos of nearby giant galaxies (M 84, M 86, M 87) based on the $r^{1/4}$ law, using data from Peletier *et al.* (1990) and Caon *et al.* (1990), gives such a low blue surface brightness in our selected field (fainter than 31 mag arcsec^{-2}) that no detection of PNs belonging to those galaxies can be expected. For comparison, in Section 6 we derive a blue surface brightness of 28.3 mag arcsec^{-2} for the detected stellar intracluster population.

The observations were made with the Prime Focus CCD camera of the 4.2m William Herschel telescope (Observatorio del Roque de los Muchachos, La Palma, Spain) on the 5-8 of May, 1997. We used a 2k $\times$ 2k Loral CCD with 15 μm pixels (0.26 arcsec pixel^{-1}) and 95% quantum efficiency at 5000 Å. The on-band and off-band interference filters were provided by the Instituto de Astrofísica de Canarias (IAC filters numbers 7 and 18): their central wavelengths were 5028 Å and 5457 Å, maximum transmissions 87% and 77%, equivalent widths 45.2 and 147.7 Å, and FWHMs 50 and 200 Å respectively. Since the filters were located in the f/2.8 converging beam, and the operating temperature was about 12°C, the central wavelengths were blueshifted to 5021 Å and 5450 Å, for the on- and off-band filter. For the mean redshift of the Virgo cluster, and the velocity dispersion $\sigma_{\rm cluster} = 800$ km s^{-1} the width of the on-band filter covered all the velocities in the $-2.6\sigma_{\rm cluster}$ to $+1.2\sigma_{\rm cluster}$ range, centered at the mean redshift of the Virgo cluster. The interference filters were smaller than the normal filters used at the WHT Prime Focus camera, and the effective surveyed field was circular with a radius of 4 arcmin. We had sporadic cirrus clouds during the first two nights; the third night was photometric. The typical seeing was 0.9 arcsec, and 1.1 arc sec at large airmasses.

We were able to make 10 $\times$ 3600 s exposures through the on-band filter, with air

masses less than 1.4, and 8×1500 s exposures through the off-band filter (frequently at higher air masses). We reached a fainter limiting magnitude in the off-band images. We also obtained on-band and off-band exposures of the standard star G138-31 (Oke 1990) for the flux calibrations, and several twilight flat fields with high number counts.

The CCD reductions were made using standard tasks provided by IRAF[2]. After bias-level subtraction and flatfielding, the on-band images were registered and combined, to minimize the effect of bad columns (the telescope was dithered between exposures) and eliminate cosmic ray events. The image combination was made with the IRAF task COMBINE, using the AVERAGE option and CCDCLIP rejection (pixel rejection based on CCD noise parameters).

3. Detections and photometry

The resulting combined on- and off-band images were split into subimages, and each of the 16 on-band subimages was carefully inspected for PN [O III] emission by blinking it with the corresponding off-band subimage. A test image obtained by dividing the on-band image by the off-band image was also blinked with the off-band image. With these two blinking procedures, several candidates were selected. For each candidate we inspected the individual images, to check whether the apparent emission was an artifact resulting from the bad CCD columns or from an uneliminated partial superposition of cosmic ray events (a few such cases were found). After careful examination, we identified 11 PN candidates which satisfied the following criteria:

---

[2]IRAF is distributed by the National Optical Astronomical Observatories, operated by the Association of Universities for Research in Astronomy, Inc., under contract to the National Science Foundation of the U.S.A.

(1) they were clearly visible (detection above 2.5 sigma) in the combined on-band image, but not visible (below 1 sigma) in the combined off-band image,

(2) of similar brightness in all of the individual on-band images,

(3) unresolved point-like sources.

Two additional unresolved sources were found: although they appear much brighter in the on-band image, they are also visible in the off-band image. We will discuss them below in more detail.

Arnaboldi *et al.* (1996) found 3 intergalactic PNs in an area of 16 arcmin^2, which would imply the presence of 9 PNs in our 50 arcmin^2 field, if we assume a similar PN surface density and the same limiting magnitude. Therefore we find good agreement between the detected candidates and the expected number of intracluster PNs from the previous work. This agreement is relevant in particular because the 3 intergalactic PNs of Arnaboldi *et al.* are spectroscopically confirmed.

The photometry was made with the PHOT and DAOPHOT routines in IRAF, following standard procedures: aperture photometry for the standard star (an aperture diameter of 14 pixels was adopted) and PSF-fitting for all point sources in the on-band and off-band combined images. The FWHM of the PSF was 4 and 5 pixels for the combined on-band and off-band images, respectively; the larger FWHM for the off-band image was expected because of the larger air masses. A set of 20 stars was used (1) to calculate an aperture correction of -0.23 mag to the instrumental magnitudes, and (2) to correct the instrumental magnitudes from the first two (non-photometric) nights to the system of the images from the last (photometric) night. This correction was -0.14 mag.

We obtained the fluxes I_{5007} in erg cm^{-2} s^{-1}, using the measurements of the standard star G138-31 and the properties of the on-band filter. The I_{5007} flux can be expressed in

magnitudes m_{5007},

$$m_{5007} = -2.5\,\log(I_{5007}) - 13.74 \tag{1}$$

(Jacoby 1989). The m_{5007} of the 11 PN candidates are between 26.8 and 28.6. We estimate errors of 0.05 mag for the brighter objects and 0.2 mag for the fainter ones.

4. Emission-line galaxies?

Could our objects be unresolved emission-line galaxies whose emission lines have been redshifted into the on-band filter centered at 5021 Å (e.g. [O II] 3727 at $z = 0.35$, or Lyman α at $z = 3.1$) ? We can estimate how many high-redshift emission-line galaxies would lie within our field of 50 arcmin^2. From our photometry, an object must be fainter than 26th (visual) magnitude to be undetected in our off-band combined image. We can use the analysis of Ellis *et al.* (1996) and Heyl *et al.* (1997) on high redshift starburst galaxies as a starting point for our discussion. We assume that $H_0 = 70$ km s^{-1} Mpc^{-1} and $q_0 = 0.5$. Then, for redshifts between 0.340 and 0.354, from eqs. (6), (7), (8) of Ellis *et al.*, we find that the proposed starburst galaxies must be fainter than $M_{b_j} = -16$, and that the effective surveyed volume is 228 Mpc^3. From Figure 21 of Heyl *et al.*, we read a value of 0.022 galaxies Mpc^{-3} mag^{-1} for the luminosity function of starburst galaxies. For our surveyed volume of 228 Mpc^3 we derive a total number of 5 starburst galaxies per mag. Even if these galaxies were to appear unresolved in the on-band image, their [O II] 3727 emission would need to be very strong to satisfy our observational constraints. From our filter transmission curves, if these high redshift galaxies have a $m_{5007} \sim 28$, and remain undetected in the off-band image, then their [O II] 3727 equivalent width has to be 100 Å. Figure 19 of Heyl *et al.* indicates that the [O II] equivalent widths of these high redshift galaxies do not usually

reach this level. Additional evidence comes from studies of emission-line galaxies detected by Popescu *et al.* (1996). From unpublished spectra it is possible to estimate that only about 5% of those emission-line galaxies can have an [O II] equivalent width of 100 Å.

We conclude that none of our PN candidates brighter than $m_{5007} \sim 28$ can be explained as starburst galaxies at $z = 0.35$, perhaps only a few of the fainter ones. From similar arguments (see also Theuns and Warren 1997) we can also exclude galaxies or quasars at higher redshifts as an explanation for the majority of our PN candidates.

Some level of contamination remains possible in our sample, and we plan to acquire spectra of our PN candidates in the near future. It seems likely that the two point-like sources reported above, which were visible in the off-band image and brighter in the on-band, are starburst galaxies or quasars; this also requires spectroscopic confirmation.

5. The cumulative PN luminosity function

In what follows we will assume that the 11 candidates are intergalactic PNs in the Virgo cluster. The sample is limited, so we cannot build the PN luminosity function as in Jacoby *et al.* (1990). We prefer to use the cumulative PN luminosity function, which gives for each value of m_{5007} the total number of PNs brighter than m_{5007}.

The result is given in Figure 1, where the cumulative PNLF is compared with simulated PNLFs. The simulated PNLFs are calculated for three different sample sizes (by sample size we mean the total number of PNs in the surveyed area, of which only the brightest are detected). We use numerical PNLF simulations like those discussed by Méndez and Soffner (1997). These PNLF simulations reproduce the observed PNLF of M 31's bulge, a population without recent star formation, assumed to be sufficiently similar to the one in the outskirts of elliptical galaxies.

To transform the measured m_{5007} into absolute magnitudes, we adopt a distance modulus of 30.9 mag and an interstellar extinction correction of 0.06 mag (Jacoby *et al.* 1990, Méndez *et al.* 1993). The simulated and observed cumulative PNLFs agree well, which supports the identification of our candidates as intracluster PNs in the Virgo cluster. We do not have enough objects for a reliable distance determination, but the good agreement between the observed and simulated PNLFs is a check of consistency with the adopted distance modulus.

6. The surface mass density of the diffuse population

From our rough evaluation of the PNLF sample size in Figure 1, we estimate the surface mass density of the diffuse intergalactic population.

If $\dot{\xi}$ is the specific PN formation rate, in PN yr^{-1} L$_{\odot}^{-1}$; $L_{\rm T}$ is the total bolometric luminosity of the sampled population; and $t_{\rm PN}$ is the lifetime of a PN (which we take as 30,000 years), then the PNLF sample size $n_{\rm PN}$ is given by the following relation:

$$n_{\rm PN} = \dot{\xi}\ L_{\rm T}\ t_{\rm PN} \tag{2}$$

For a more detailed discussion on the practical use of this relation, see Méndez *et al.* (1993) and Soffner *et al.* (1996).

Here we adopt $n_{\rm PN} = 100$, from Figure 1, and $\dot{\xi} = 4 \times 10^{-12}$ (a typical value for Virgo ellipticals, with an uncertainty of about 50%; see Jacoby *et al.* 1990 and Méndez *et al.* 1993). We derive a surveyed luminosity of 8×10^8L$_{\odot}$. Given the uncertainties in $n_{\rm PN}$ and $\dot{\xi}$, we estimate that our result for the surveyed luminosity is uncertain by a factor 2 or 3.

Would this intracluster population be detectable through its emitted continuum light?

The luminosity derived above ($8 \times 10^8 L_\odot$) corresponds to a blue surface brightness of 28.3 mag arsec^{-2}, which would be difficult to detect on the angular scale of the Virgo cluster. We conclude that there is no inconsistency at this time between the diffuse surface brightness of the Virgo cluster and the presence of an intracluster stellar population as seen through the PNs.

Binggeli *et al.* (1987) estimate that the central surface luminosity density in the Virgo cluster is $10^{11} L_\odot \mathrm{deg}^{-2}$. This is equivalent to $1.4 \times 10^9 L_\odot$ in our surveyed area of 50 arcmin^2. Therefore, assuming similar distributions, the luminosity contributed by the intracluster population could be of the order of 50% of the luminosity from all galaxies in the Virgo cluster. This number is quite similar to that found by Theuns and Warren (1997) in the Fornax cluster and by Bernstein *et al.* (1995, from a study of the diffuse light) in the Coma cluster.

Assume now for the Virgo intracluster stars a mass-to-luminosity ratio of 5, typical for the stellar content of an old population (we do not include here any dark matter possibly associated with such a population). Then the total surveyed stellar mass is 4×10^9 $M_\odot$. Again, this could amount to about 50% of the stellar mass from all galaxies in the cluster. At a distance of 15 Mpc our surveyed area corresponds to 10^9 pc^2. Therefore the surface mass density of stars is 4 $M_\odot \mathrm{pc}^{-2}$ for the intracluster population at the surveyed position.

Let us compare the intracluster stellar surface mass density of 4 $M_\odot \mathrm{pc}^{-2}$ with the surface mass density of the total gravitational mass in the Virgo cluster at the same position in the sky. A rough estimate of the latter can be obtained as follows. We take recent studies of the Virgo cluster structure as derived from X-ray images (Böhringer *et al.* 1994) and X-ray spectra (Nulsen and Böhringer 1995). We adopt the distribution of gravitating mass given by Nulsen and Böhringer (see their Eq. 13 and their Fig. 5), extrapolate it out to a distance of 1 Mpc from the center of M 87 (which gives a total gravitating mass of 1.5×10^{14}

solar masses), recover the mass density (mass per unit volume) at each point and integrate along the line of sight through the cluster at the position of our field. In this way we obtain a total gravitational surface mass density of 80 $M_{\odot}pc^{-2}$. Since the surface L density of the intracluster population is $8 \times 10^{8} \times 10^{-9} L_{\odot}pc^{-2}$, we conclude that the M/L ratio (where M is the total gravitational mass) at the position of our search is approximately 100.

Nulsen and Böhringer estimate that the total gravitational mass near the center of the cluster is roughly 15 times the mass of the hot gas. We obtain a similar factor (20) for the ratio between the total gravitational mass and the mass of the intracluster population. Then, if we assume spherical symmetry and similar distributions as a function of distance to the center, the mass of the diffuse intracluster stellar population may be of the same order of magnitude as the mass of hot gas in the intracluster medium.

All these estimates are of course extremely uncertain, and our main purpose in making them is to show that it would be interesting to repeat the search for PNs at several different positions across the Virgo cluster in order to map the surface mass density of the diffuse intracluster population. The contribution from this new population cannot account for all the dark matter in the Virgo cluster, but it certainly increases the ratio of visible to total matter, making it harder to reconcile the results of standard big bang nucleosynthesis with an $\Omega_0 = 1$ universe, as discussed for example in White *et al.* (1993).

7. Conclusions

Our search confirms our earlier discovery of an intracluster stellar population in the Virgo Cluster, and gives a further hint that this population may represent a significant contribution to the total mass of the cluster. The next steps in this program are: (1) survey further fields at different distances from the center of the cluster, to map the structure of

this population; (2) acquire spectra of the detected objects, to check their identification as PNs and to start the kinematical study of this population; (3) study numerical simulations of star stripping, scaled to the Virgo Cluster, to investigate the expected kinematics of the stripped stellar population and to evaluate the likely mass fraction of stripped stars in the cluster.

The William Herschel Telescope is operated on the island of La Palma by the Isaac Newton Group in the Spanish Observatorio del Roque de Los Muchachos of the Instituto de Astrofísica de Canarias. The work reported here has been supported by the Deutsche Forschungsgemeinschaft through Grant SFB (Sonderforschungsbereich) 375. RHM would like to acknowledge useful discussions with Ralf Bender and Roberto Saglia.

REFERENCES

Arnaboldi M., Freeman K.C., Méndez R.H. *et al.* 1996, ApJ, 472, 145

Bernstein G.M., Nichol R.C., Tyson J.A., Ulmer M.P., Wittman D. 1995, AJ, 110, 1507

Binggeli B., Tammann G.A., Sandage A. 1987, AJ, 94, 251

Böhringer H., Briel U.G., Schwarz R.A., Voges W., Hartner G., Trümper J. 1994, Nature, 368, 828

Caon N., Capaccioli M., Rampazzo R. 1990, A&AS, 86, 429

Drinkwater M.J., Currie M.J., Young C.K., Hardy E., Yearsley J.M. 1996, MNRAS, 279, 595

Ellis R.S., Colless M., Broadhurst T., Heyl J., Glazebrook K. 1996, MNRAS, 280, 235

Ferguson H., Tanvir N., von Hippel T. 1996, BAAS, 28, 1382

Ferguson H., Tanvir N., von Hippel T. 1997, Nature (submitted)

Heyl J., Colless M., Ellis R.S., Broadhurst T. 1997, MNRAS, 285, 613

Jacoby G.H. 1989, ApJ, 339, 39

Jacoby G.H. 1997, in IAU Symp. 180 (Planetary Nebulae), in press

Jacoby G.H., Ciardullo R., Ford H.C. 1990, ApJ, 356, 332

Méndez R.H., Kudritzki R.P., Ciardullo R., Jacoby G.H. 1993, A&A, 275, 534

Méndez R.H., Soffner T. 1997, A&A, 321, 898

Moore B., Katz N., Lake G., Dressler A., Oemler A. 1996, Nature, 379, 613

Nulsen P.E.J., Böhringer H. 1995, MNRAS, 274, 1093

Oke J.B. 1990, AJ, 99, 1621

Peletier R.F., Davies R.L., Illingworth G.D., Davis L.E., Cawson M. 1990, AJ, 100, 1091

Popescu C.C., Hopp U., Hagen H.J., Elsässer H. 1996, A&AS, 116, 43

Soffner T., Méndez R.H., Jacoby G.H., Ciardullo R., Roth M.M., Kudritzki R.P. 1996, A&A, 306, 9

Theuns T., Warren S.J. 1997, MNRAS, 284, L11

White S.D.M., Navarro J.F., Evrard A.E., Frenk C.S. 1993, Nature, 366, 429

This manuscript was prepared with the AAS LaTeX macros v4.0.

Fig. 1.— The cumulative PNLF (full line) derived from our sample of 11 PNs, if we assume them to be at the distance of the Virgo cluster, and if we adopt a distance modulus of 30.9. For comparison, we show three simulated PNLFs, which represent typical PN populations like those found in early-type Virgo cluster galaxies or in the bulge of M 31. These three simulated PNLFs (dashed lines) were calculated for a maximum final mass of 0.63 $M_\odot$ and sample sizes of 50, 100 and 150 PNs. For details, see Méndez and Soffner (1997). From the comparison of the observed cumulative PNLF with the simulated ones we estimate a sample size of about 100 PNs for our Virgo intergalactic PNs.

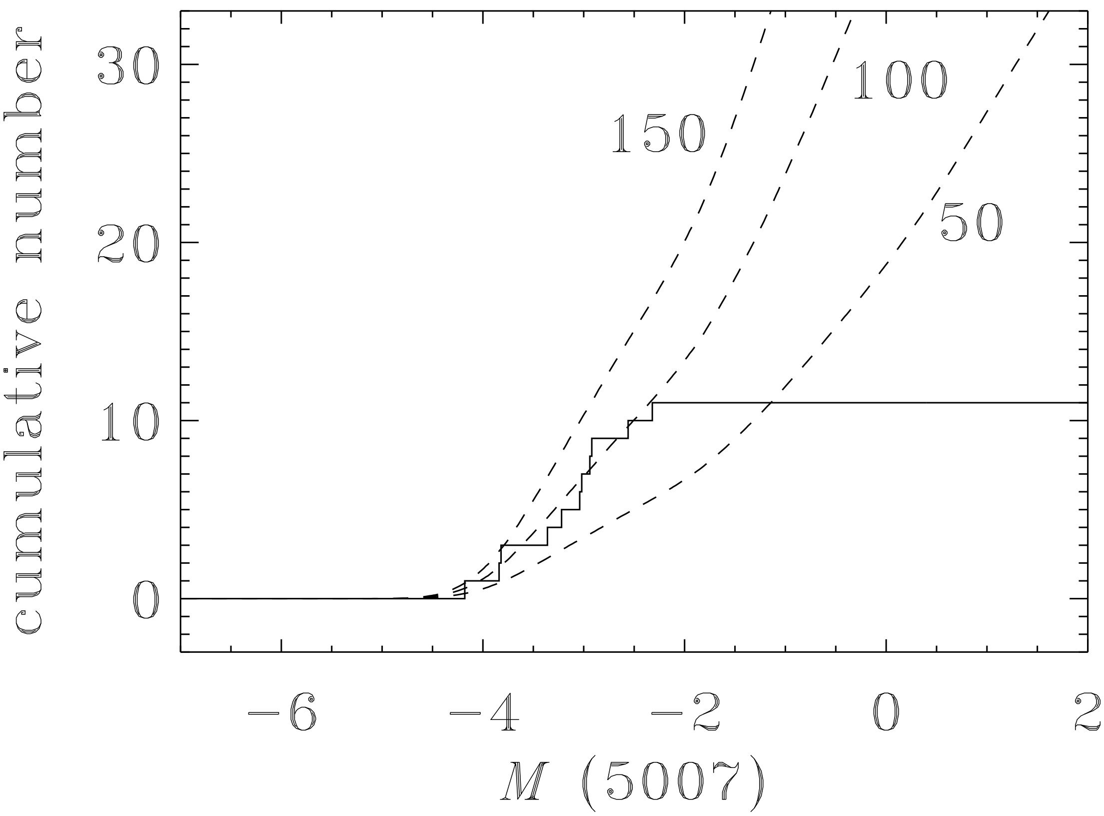
cumulative number
30
20
10
0
150
100
50
−6
−4
−2
0
2
M (5007)